LARGE EDDY SIMULATION OF VORTEXING FLOW IN THE MOLD WITH DC MAGNETIC FIELD

Qian Zhongdong[1*] and Wu Yulin[2]

Large eddy simulation of vortexing flow of molten steel in the continuous casting mold with and without DC magnetic field was conducted. The influence of the position of magnetic field to the residence time and depth of the vortex was analyzed. The mechanism of the influence of magnetic field to the vortexing flow was found. The computational results show that the vortexing flow is the result of shearing of the two un-symmetric surface flows from the mold narrow faces when they meet adjacent to the SEN; the un-symmetric flow for turbulent vortex is caused by turbulent energy of the fluid and that for biased vortex is caused by biased flow and the turbulent energy of fluid; with the moving of the magnetic field from the centerline of the outlet of the SEN to the free surface, the surface velocity is decreased gradually and the depth of the turbulent vortex and the biased vortex is decreased, the residence time is increased with the magnetic field moves from DL=120mm to DL=60mm and then decreased; the turbulent vortex and the biased vortex can be eliminated when the magnetic field is located at the free surface.

Keywords: Continuous Casting, Electromagnetic Braking, Vortexing Flow

The molten steel flow in a mold for continuous casting is unstable, and vortexing flow exists in the free surface. It is believed to be a significant contribution to mold powder entrapment; the entrapped flux may be carried deeply into the mold by the vortexing flow and results in the uncleanness of the steel. Water modeling studies by Li have reveled the existence of the vortex in the mold adjacent to the submerged entry nozzle (SEN) even when the SEN is located at the centerline of the mold.[1] He[2] concluded that the existence of vortex in the mold was the result of biased flow between the SEN ports, generated by effects of the slide gate, nozzle clogging, turbulent flow, etc. It is found that most of the inner defects appear around the SEN, which shows that the vortexing flow is a significant caution to mold powder entrapment and inner defects of slab.[1,3]

Water modeling studies are most widely adopted in the research of vortexing flow in mold. Li[3] simulated the "biased vortex" (the vortex with off-center SEN) by the k-εtwo-equation model, however, the "turbulent vortex" (the vortex with center SEN) was not mentioned. Qian[4] simulated the "turbulent vortex" and the "biased vortex" using the LES (large eddy simulation) model and designed a new vortex brake to eliminate the vortex in mold, however, the biased vortex can not be eliminated by the vortex brake, though it can be suppressed significantly. In this study, the vortexing flow with DC magnetic field is simulated. The relationship between the location of the magnetic field and some characters of the vortexing flow is analyzed.

Received: June 9, 2004, Accepted: Feburary 2, 2005

1. State Key Laboratory of Water Resources and Hydropower Engineering Science, Wuhan University, Wuhan, Hubei, 430072, China
2. Depatrment of Thermal Engineering, Tinghua University, Beijing 100084,China
* Corresponding Author. Email: qianzhongdong@tsinghua.org.cn

1. MATHEMATICAL MODEL

1.1 GOVERNING EQUATIONS

The LES equations are obtained by filtering Navier-Stokes equations using the top-hat filter and read[5]

$$\frac{\partial \rho}{\partial t}+\frac{\partial}{\partial x_i}(\rho \overline{u}_i)=0 \tag{1}$$

$$\frac{\partial \overline{u_i}}{\partial t}+\frac{\partial}{\partial x_j}\left(\overline{u_i u_j}\right) = -\frac{1}{\rho}\frac{\partial \overline{p}}{\partial x_i}+\frac{\partial}{\partial x_j}\left\{v\left(\frac{\partial \overline{u_i}}{\partial x_j}+\frac{\partial \overline{u_j}}{\partial x_i}\right)+\tau_{ij}\right\}+\frac{1}{\rho}F_i \quad (2)$$

Where the subgrid-scale (SGS) stress tensor $\tau_{ij}=2v_t\bar{S}_{ij}+\frac{1}{3}\tau_{ll}\delta_{ij}$ and the resolved strain-rate tensor read

$$\bar{S}_{ij}=\frac{1}{2}\left(\frac{\partial \overline{u_i}}{\partial x_j}+\frac{\partial \overline{u_j}}{\partial x_i}\right) \quad (3)$$

The eddy viscosity $v_t=(C_s\Delta)^2\left|\bar{S}_{ij}\right|$, where $\left|\bar{S}_{ij}\right|=\sqrt{2\bar{S}_{ij}\bar{S}_{ij}}$ and C_s is the Smagorinsky coefficient. In this study C_s=0.1 is adopted. $\vec{F}$ is the electromagnetic force.

1.2 CALCULATION OF ELECTROMAGNETIC FORCE

The electric current density induced in the moving conducting fluid under DC magnetic field is given by the Ohm's equation[6]

$$\vec{J}=\sigma(\vec{E}+\vec{u}\times\vec{B}) \quad (4)$$

In the foregoing equation, electric field intensity $\vec{E}$ can be expressed as gradient of electric potential φ. Then the following equation is obtained

$$\vec{J}=\sigma(-\nabla\varphi+\vec{u}\times\vec{B}) \quad (5)$$

The induced current should satisfy the continuity equation

$$\nabla\cdot\vec{J}=0 \quad (6)$$

Substitution of equation (5) into equation gives

$$\nabla\cdot(\sigma\nabla\varphi)=\nabla\cdot\sigma(\vec{u}\times\vec{B}) \quad (7a)$$

In order to simplify the calculation, the electrical conductivity σ is assumed constant and the skin effect is neglected. Therefore equation (7) can be rewritten as following

$$\nabla^2\varphi=\nabla\cdot\left(\vec{u}\times\vec{B}\right) \quad (7b)$$

The electromagnetic force is obtained by the follow equation

$$\vec{F}_m=\vec{J}\times\vec{B} \quad (8)$$

It can be found from equation (7) that the flow field is coupled with the electromagnetic field. So iteration has to be conducted until the critical standard arrived in each time step.

1.3 BOUNDARY CONDITION

The nozzle inlet velocity is calculated by transferring the casting speed. At the exit, the condition of fully developed flow is adopted, i.e., normal gradients of all variables for fluid flow are set to zero. Near the wall, empirical "wall-law" function is employed to define the Smagorinsky coefficient

Table. 1 Geometrical Parameters and Thermophysical Properties of Steel for Simulation

Parameters	Values
Mold size, mm	720(width)×60(thickness)×1500(length)
Nozzle, mm	25(thickness) ×50(width)
Depth of nozzle, L, mm	120
Port angle of nozzle, θ , °	35
Casting speed, m/min	1.5
Density of molten steel, kg/m^3	7020
Viscosity of molten steel, N·s/m^2	5.59×10^{-3}
Magnetic flux density , T	0.1
Position of magnetic flied, DL, mm	0, 30, 60, 120

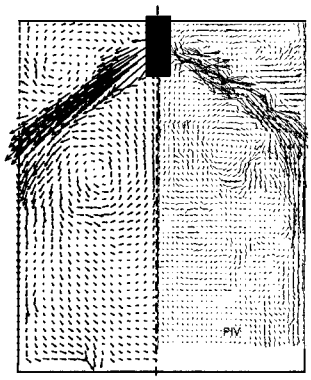

Fig. 1 Comparison of computational and experimental flow filed

$$l = C_s\overline{\Delta}[1-\exp(-y^+/26)^3]^{1/2}, \qquad (9)$$
$$\overline{\Delta} = (\Delta x\Delta y\Delta z)^{1/3}$$

Boundary condition for the electric potential used in this study is set as the following[6]
At the meniscus and mold wall

$$\nabla\varphi = (\vec{u}\times\vec{B}) \qquad (10)$$

At the end of casting direction

$$\varphi = 0 \qquad (11)$$

2. VERIFICATION OF MATHEMATICAL MODEL

In order to verify the mathematical model, the fluid flow in the experimental device designed by Thomas[7,8] is simulated. Fig. 1 shows the comparison between the computational and the experimental results. The agreement between the computational and experimental results can be seen to be excellent.

3. RESULTS AND DISCUSSION

The geometrical parameters and the thermophysical properties of steel for simulation are listed in Table. 1, Fig. 2 illustrates the structure and position of the nozzle and the position of the magnetic field in this study. A 360×30×75 rectangular grid system was used with a time step of 0.0008s. 300s flow was simulated for each operating parameter.

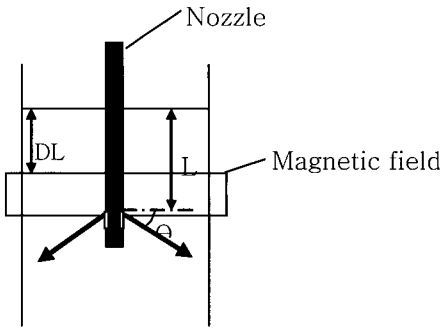

Fig. 2 Positions of the SEN and the magnetic field

Fig. 3 shows flow fields in the free surface with center nozzle. (a) is the time averaged flow field and (b)-(f) are instantaneous flow fields. It can be seen that the time averaged flow field is symmetric while the instantaneous flow fields are unsymmetric and the vortexing flow pattern in (b)-(f) varies periodically with time. The vortexing flow is the result of shearing of the two un-symmetric surface flows from the narrow face of mold when they meet adjacent to the SEN. It can be concluded from Fig. 3 that the two un-symmetric surface flows are caused by turbulent energy of the fluid, therefore, in this study the vortexing flow with center nozzle was named "turbulent vortex".

The vortex with off-center SEN, which is named "biased vortex" in this study, is another type of vortex existing in the free surface. The biased vortex with a 10mm biased distance of SEN from the mold centerline to the left-hand side was simulated in the present work. Fig. 4 shows the biased flow fields in the free surface. (a) is the time averaged flow field and (b)-(e) are the instantaneous ones. It can be seen from (a) that the biased time averaged flow field is un-symmetric and the biased vortex appeared.

It can be found from the comparison of Fig. 3(a) and Fig. 4(a) that the biased vortex is the result of shearing of the two un-symmetric surface flows caused by the biased flow when they meet adjacent to the SEN. The flow pattern of the biased vortex varies with time as shown in (b)-(e). A conclusion can be drawn from Fig. 4 that the biased vortex is caused by the biased flow and the turbulent energy of the fluid.

From the forgoing numerical analysis, the mechanism of the vortexing flow may be

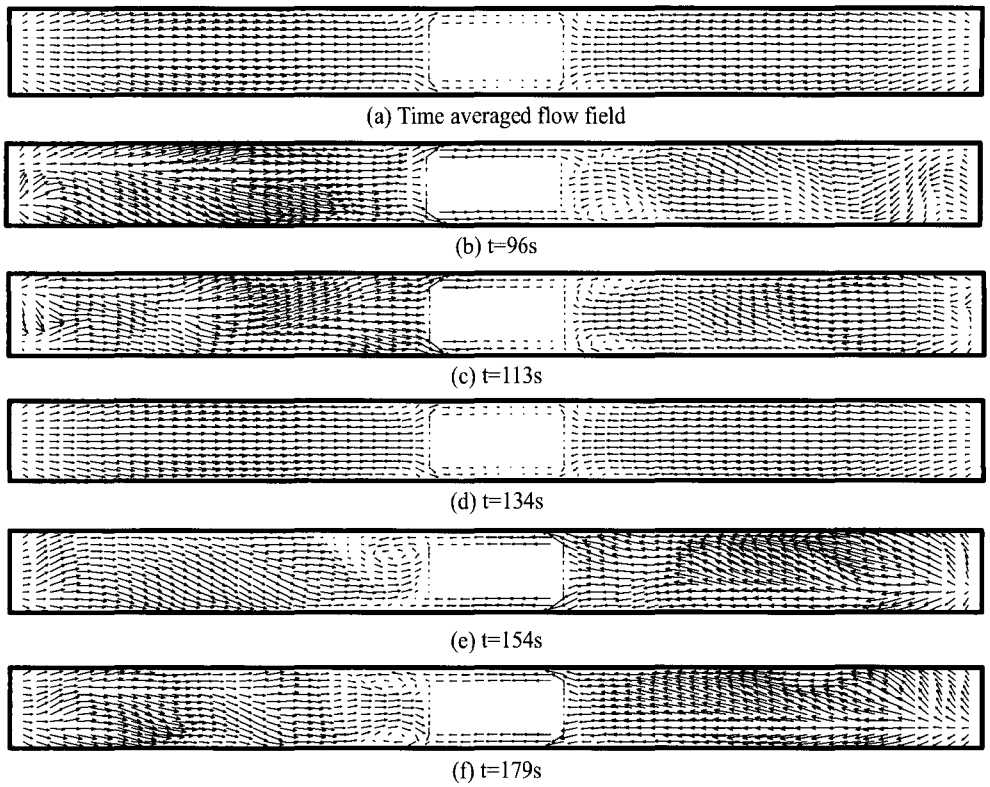

(a) Time averaged flow field

(b) t=96s

(c) t=113s

(d) t=134s

(e) t=154s

(f) t=179s

Fig. 3 Flow fields in the free surface with center nozzle without magnetic field

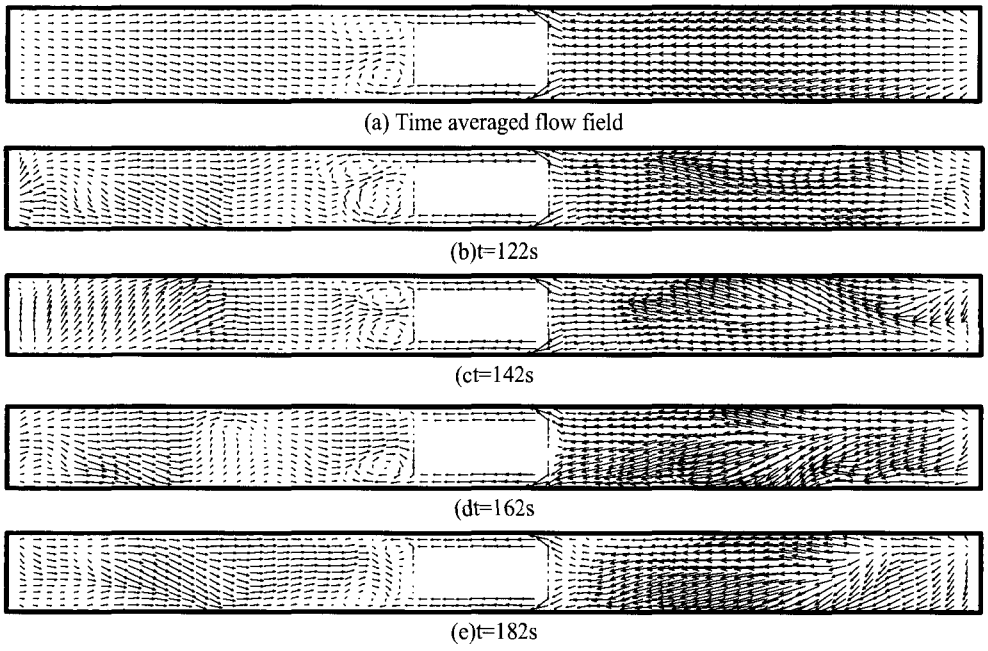

(a) Time averaged flow field

(b)t=122s

(ct=142s

(dt=162s

(e)t=182s

Fig. 4 Flow fields in the free surface with the off-center nozzle without magnetic field

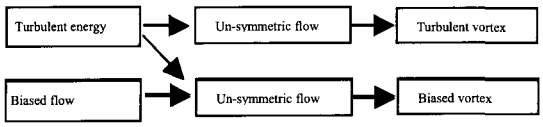

Fig. 5 Mechanism for turbulent vortex and biased vortex

summarized as follows. Vortexing is the result of shearing of the two un-symmetric surface flows from the mold narrow faces when they meet adjacent to the SEN. The unsymmetric flow for turbulent vortex is caused by turbulent energy of the fluid and that for biased vortex is caused by biased flow and the turbulent energy of fluid as shown in Fig. 5.

On the basis of the mechanism of vortexing flow, suppressing the surface velocity by EMBr (electro-magnetic brake ruler) is expected to eliminate the vortexing flow. The turbulent vortex and the biased vortex with different positions of magnetic field are simulated in this study. The residence time, the depth of the vortex and the surface velocity are considered. Fig. 6 shows the flow fields of half-thickness with center SEN with and without EMBr. Fig. 7 shows the flow fields at selected sections with center SEN with EMBr when DL=30mm. The comparison of the vortexing characters with different positions of the magnetic field is listed in Table 2.

It can be seen from Fig. 6 and Fig. 7 that the upward re-circulating flow is suppressed by the magnetic field, therefore, the surface velocity is decreased. The flow field in the magnetic field covered section is suppressed significantly and the votexing flow is eliminated. With the moving of the magnetic field from the centerline of the outlet of the SEN to the free surface, the surface velocity is suppressed gradually and the depth of the turbulent vortex and the biased vortex is decreased as shown in Table 2. When the magnetic field is located at the free surface, the turbulent vortex and the biased vortex in the free surface are almost eliminated.

The position of the magnetic field does not have linear influence on the residence time of the vortexing flow. A new model is introduced to explain the influence of the position of the magnetic field to the residence time of the vortexing flow and the surface velocity as shown in Fig. 8. The two jet flows from the outlets of the SEN and the two upward re-circulating flows are un-symmetric because of biased flow and turbulent energy of fluid, therefore, the two flows from in the free surface from the narrow side of the mold are un-symmetric. Suppression of the jet flow and the upward re-circulating flow is helpful to suppress the vortexing flow. When the magnetic field is located at the centerline of the outlet of the SEN, the jet flow and the upward re-circulating flow are

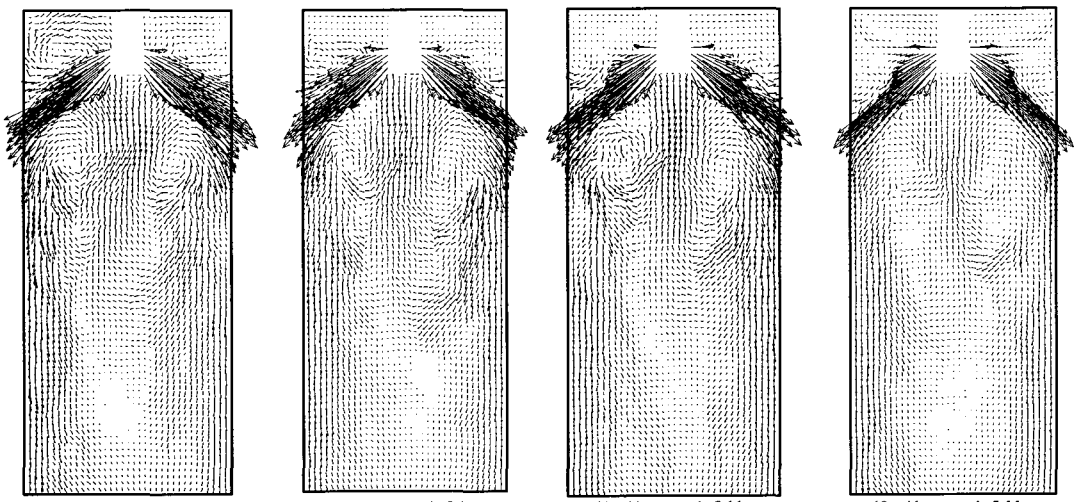

Fig. 6 Flow fields with and without magnetic field (t=100s)

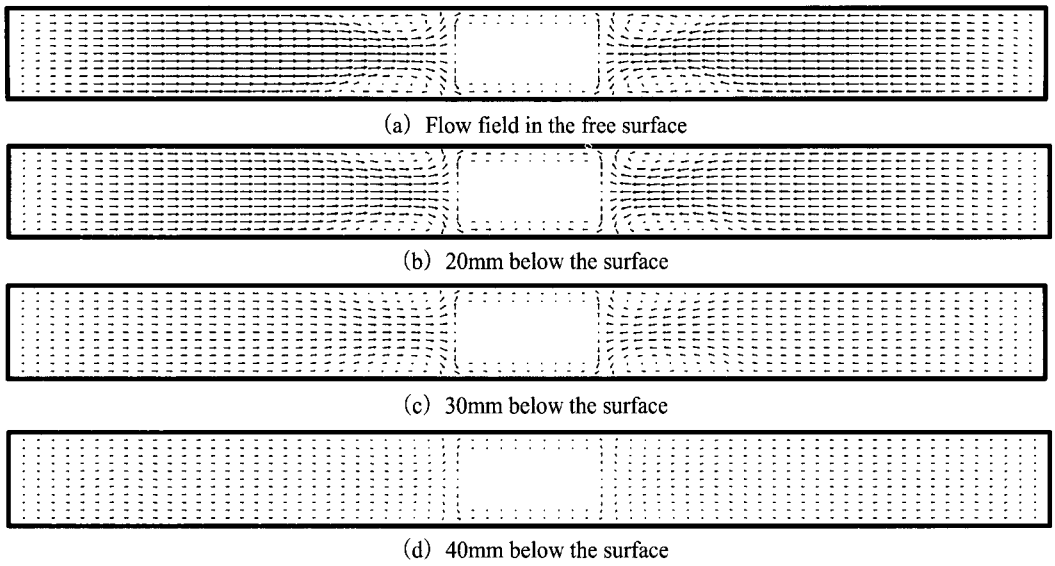

(a) Flow field in the free surface

(b) 20mm below the surface

(c) 30mm below the surface

(d) 40mm below the surface

Fig. 7 Flow fields at selected horizontal sections with magnetic field (t=100s)

suppressed, so the residence time of the vortexing flow is decreased to 102s. However, when the magnetic field moves from DL=120mm to DL=60mm, the jet flow is not suppressed and the upward flow is weakly suppressed because the direction of the stream and the induced electric current are parallel near the surface of the walls[9], therefore, the residence time of the vortexing flow is decreased only to 247.8s. When the magnetic field moves from DL=60mm to DL=30mm, the direction of the stream changes a little as shown in Fig. 8(c), so the suppression of the magnetic field to the upward flow is a little stronger. The best position of the magnetic field to suppress the vortexing flow is DL=0, where the flow in the free surface is directly suppressed by the magnetic field and the vortexing flow is suppressed significantly. It can be seen from Fig. 8(a) that a circulating flow appears above the magnetic field, therefore, the flow in the free surface is composed of the circulating flow, which is symmetric as shown in Fig. 7(d), and the upward re-circulating flow, that is why the surface velocity with DL=120mm is larger than that with DL=60mm. The mechanism of the vortexing flow is also proved by Fig. 8(a) that only the un-symmetric component of flow in the free surface is contribution to the vortexing flow.

4. CONCLUSIONS

(1) Vortexing flow is the result of shearing of the two un-symmetric surface flows from the mold narrow faces when they meet adjacent to the SEN. The un-symmetric flow for turbulent vortex is caused by turbulent energy of the fluid and that for biased vortex is caused by biased flow and the turbulent energy of fluid.

(2) With the moving of the magnetic field from the centerline of the outlet of the SEN to the free surface, the surface velocity is decreased gradually

Table. 2 Comparison of vortexing characters with different positions of magnetic field

	Turbulent vortex					Biased vortex	
	Without EMBr	DL=120mm	DL=60mm	DL=30mm	DL=0mm	Without EMBr	DL=0mm
Residence time, s	250	102	247.8	237.6	6	296	7
Depth, mm	120	120	70	40	10	120	10
Velocity, m/s	0.0372	0.0244	0.0179	0.0084	0.0063	0.0535	0.0083

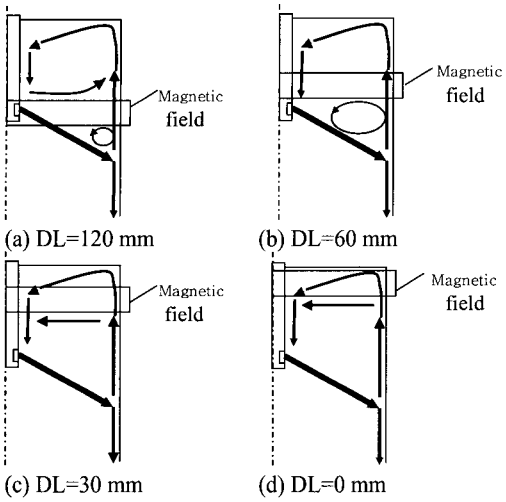

Fig. 8 Influence of the position of magnetic field to the residence time of vortex flow

and the depth of the turbulent vortex and the biased vortex is decreased, the residence time is increased with the magnetic field moves from DL=120mm to DL=60mm and then decreased.

(3) The best position of the magnetic field to suppress the vortexing flow is DL=0, where the flow in the free surface is directly suppressed by the magnetic field and the vortexing flow is suppressed significantly.

ACKNOWLEDGEMENTS

This study was funded by Open Research Fund Program of State Key Laboratory of Water Resources and Hydropower Engineering Science under the contact No.2004C006 and the National Natural Science Foundation of China under the contact No.50176022.

REFERENCES

[1] Li, B.K. and Li, D.H., 2002, "Water model observation and numerical simulation of vortexing flow at molten steeling surface in continuous casting mold," *Acta Metallurgica Sinica*, 38(3), pp.315-320.

[2] He, Q.L., 1993, "Observations of vortex formation in the mould of a continuous slab caster," *ISIJ Inter*, 33, pp.343-345.

[3] Li, B.K., Okane, T. and Umeda, T., 2001, "Modeling of biased flow phenomena associated with the effects of static magnetic-field application and argon gas injection in slab continuous casting of steel," *Meatllurgical and Meterials Transaction B*, 32, pp.1053- 1066.

[4] Qian, Z. and Wu Y., 2003, "Large eddy simulation and controlling of vortexing flow of molten steel in continuous casting mold," *The 5th asian computational fluid dynamics*, BUSAN, KOREA.

[5] Moin, P. and Kim, J., 1982, "Numerical investigation of turbulent channel flow," *J Fluid Mech.*, pp.341-377.

[6] Qian, Z. D., Wu, Y. L., Li, B.W. and He, J. C., 2002, "Numerical Analysis of the influences of Operational Parameters on the Fluid Flow in Mold with Hybrid Magnetic Fields," *ISIJ Int.*, 42 (11), pp.1259-1265.

[7] Thomas, B. G., Yuan, Q., Sivaramakrishnan, S., et al., 2001, "Computation of four method to evaluate fluid velocities in a continuous slab mold," *ISIJ Inter*, 41, pp.1262-1271.

[8] Thomas, B. G., Zhang, L. F., 2001, "Mathematical modeling of fluid flow in continuous casting," *ISIJ Inter*, 41, pp.1181-1193.

[9] Huang, Y.S., Cha, P.R., Nam, H.S., Moon, K.H. and Yoon, J.K., 1997, "Numerical analysis of the influence of operational parameters on the fluid flow and meniscus shape in slab caster with EMBR," *ISIJ Int.* 37(7), pp.659-667.